International Journal of Electronics and Communication Engineering.
ISSN 0974-2166 Volume 4, Number 1 (2011), pp.131-138

http://www.irphouse.com

Circular Array of Tapered Nylon Rod Antennas: A Computational Study

R.V. Satyanarayana[1] and M.V.S. Prasad[2]

[1]Professor of ECE, Sri Venkateswara University College of Engineering, Tirupati-517502, A.P., India
[2]Asst. Professor, Dept. of ECE, R.V.R. & J.C. College of Engineering, Guntur-522019, A.P., India
E-mail: v.s.ravinutala@gmail.com, mvs_prasad67@yahoo.co.in

Abstract

In this paper the computational studies were performed on circular arrays using tapered Nylon (ε_r =3) dielectric rod antennas, of length (L) equal to $6\lambda_0$ and taper angle (θ_1) equal to 2.5°, as elements are presented. The objective of the computational study is to find the optimum choice of number of elements in the array. The antennas are uniformly spaced around the circumference of a circle. The number of radiating elements in the array is varied from 8 to 28, with an increase of 4 elements. The principal plane patterns are computed, using the principle of pattern multiplication. For each set of elements, Half Power Beam Width (HPBW), Side Lobe Level (SLL), and Directivity (D_0) are determined. The principle plane patterns and 3D patterns are presented for the optimum choice of elements.

Keywords: Nylon rod antenna, Circular array, Array factor, Directivity, Side Lobe Level, Half Power Beam Width.

Introduction

In a circular array, the radiating elements are placed along the circumference of a circle with uniform spacing. These arrays find wide applications in radio direction finding, air and space navigation, radar and sonar systems [1]. Several investigations has been carried out using circular arrays using with different types of radiating elements and are reported in literature [2]-[5]. An important feature of the circular array that is seen in most of the applications is the scanning of the main beam through 360° in the azimuthal plane (plane of the array). However, by proper choice of the elements, their orientation and phase excitation it is possible to obtain a main beam in the direction of zenith and scan it over a small angle cone, around the zenith direction, with a little change of either beam width or side lobe level. The choice of Nylon rod antenna of length $6\lambda_0$ and taper angle 2.5°, is made on the basis of the results of computational studies, carried out on the radiation patterns of tapered Nylon rod antennas, reported in [6]. In this paper, the results of computational studies of the radiation patterns, of a circular array of tapered Nylon dielectric rod antennas are presented.

Radiation from Tapered Nylon rod antenna

The radiation from a dielectric rod antenna mainly depends on the dielectric material used to fabricate the antenna, physical shape of the antenna, and the method of excitation of the antenna. The dielectric rod antenna is excited in the hybrid HE_{11} mode. The advantage of asymmetric HE_{11} mode is that it gives maximum radiation in the axial direction and it does not shows any cut off behavior.

The amplitude of side lobes and back lobes may be reduced, by tapering the dielectric rod antenna, until the diameter is reached for which the wave impedance becomes equal to that of free space impedance. Tapering the dielectric rod minimizes the standing wave distribution caused by reflection at the free end of the rod and the electric field distribution rises to maximum near the mid point of the length of the rod and then falls off towards the free end [7].

The electric fields radiated by a tapered dielectric rod antenna are analyzed by Anand Kumar and Rajeswari Chatterjee using the Schelkunoff's equivalence principle [8]. The principle states that the electromagnetic field inside a surface S, due to sources outside the surface can be produced by sheet electric currents J and sheet magnetic currents M over the surface S given by the following equations,

$$\mathbf{J} = -\hat{\mathbf{n}} \times \mathbf{H}^{\circ} \tag{1}$$

$$\mathbf{M} = \hat{\mathbf{n}} \times \mathbf{E}^{\circ} \tag{2}$$

where $\hat{\mathbf{n}}$ is a unit normal vector directed outwards from S, $\mathbf{E}^{\circ}$ and $\mathbf{H}^{\circ}$ are the values of E and H on the surface S. The geometry of tapered dielectric rod is shown in Fig.1. Following the analysis in [8], the electric field components radiated by a tapered dielectric rod are given by:

$$\begin{aligned}\left(\frac{2\lambda_0 r}{A}\right) j\exp(j\beta_0 r)E_\theta = & -j(1/f\varepsilon_1)\sin\phi\, I_1 + j(1/2f\varepsilon_1)\cos\phi\sin 2\phi\, I_2 \\ & - j(\lambda_0/2)\cos\theta\cos\phi\sin 2\phi\, I_3 \\ & - j\lambda_0\cos\theta\sin\phi\, I_4 + j2\pi\eta_0\sin\theta\sin\phi\, I_6 \\ & - \pi((1+\delta_1\eta_1^e) + [(\beta_1/\beta_0) + \eta_0\delta_1]\cos\theta)\exp(j\beta_1 l)\sin\phi\, I_7 \\ & - \pi((1-\delta_1\eta_1^e) + [(\beta_1/\beta_0) - \eta_0\delta_1]\cos\theta)\exp(j\beta_1 l)\sin\phi\, I_8\end{aligned} \tag{3}$$

and

$$\left(\frac{2\lambda_0 r}{A}\right) j\exp(j\beta_0 r) E_\phi = -j(1/f\varepsilon_1)\cos\theta\cos\phi I_1 - j(1/2f\varepsilon_1)\cos\theta\sin\phi\sin2\phi I_2 + j(\lambda_0/2)\sin\phi\sin2\phi I_3 - j\lambda_0\cos\phi I_4 + j2\pi\sin\theta\cos\phi I_5 + \pi((1+\delta_1\eta_1^e)\cos\theta + [(\beta_1/\beta_0)+\eta_0\delta_1])\exp(j\beta_1 l)\cos\phi I_7 + \pi((1-\delta_1\eta_1^e)\cos\theta + [(\beta_1/\beta_0)-\eta_0\delta_1])\exp(j\beta_1 l)\cos\phi I_8 \quad (4)$$

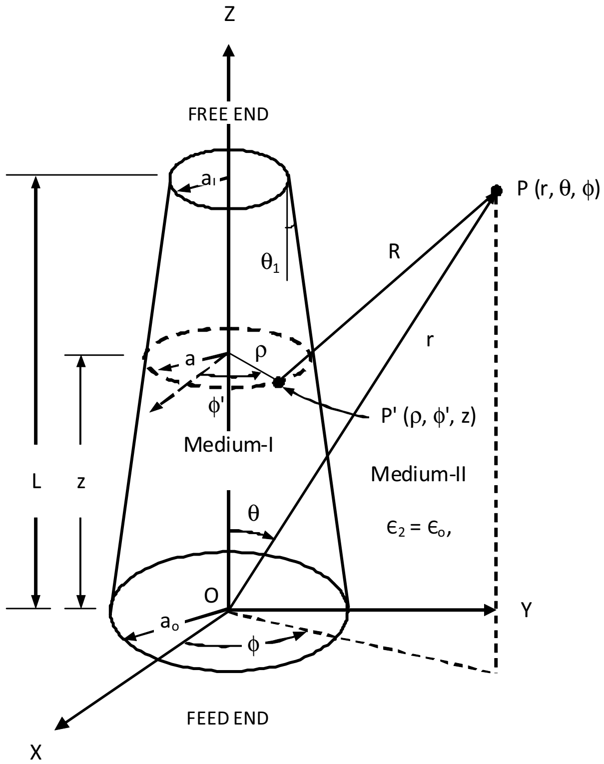

Figure 1: Geometry of tapered dielectric rod antenna.

where A is the excitation constant for H modes and

$$I_1 = \int_0^L \exp(j\beta z)\ \delta\, rJ_1(r)\left\{\sin^2\phi\, J_o(\xi) + \cos2\phi[J_1(\xi)/\xi]\right\} dz \quad (5)$$

$$I_2 = \int_0^L \exp(j\beta z)\,\delta\, k_1 rJ_1(r)\left[2\frac{J_1(\xi)}{\xi} - J_0(\xi)\right] dz \quad (6)$$

$$I_3 = \int_0^L \exp(j\beta z)\, k_1 rJ_1(r)\left[2\frac{J_1(\xi)}{\xi} - J_0(\xi)\right] dz \quad (7)$$

$$I_4 = \int_0^L \exp(j\beta z)\, k_1 r J_1(r)\left[\cos^2\phi\, J_0(\xi) - \cos 2\phi\, \frac{J_1(\xi)}{\xi})\right] dz \tag{8}$$

$$I_5 = \int_0^L \exp(j\beta z)\left[rJ_0(r) - (1-\delta\eta_1^e)J_1(r)\right]J_1(\xi)\, dz \tag{9}$$

$$I_6 = \int_0^L \exp(j\beta z)\left[\delta r J_0(r) + \left(\frac{1}{\eta_1^m} - \delta\right)J_1(r)\right]J_1(\xi)\, dz \tag{10}$$

$$I_7 = \int_0^{a_1} R\, J_0(R)\, J_0(\xi_1)\, d\rho \tag{11}$$

$$I_8 = \int_0^{a_1} [2J_1(R) - RJ_0(R)]\left[2\frac{J_1(\xi_1)}{\xi_1} - J_0(\xi_1)\right] d\rho \tag{12}$$

with $\xi = \beta_o\, a \sin\theta$ and $\xi_1 = \beta_o\, \rho \sin\theta$

In (3) - (10), δ is the ratio of excitation constants for E and H modes. The values of δ and k_1 may be computed, by representing their variation given in Fig.2 of [8], by piecewise linear models as:

$$\delta = 0.007 \text{ for } a/\lambda_0 \le 0.1 \tag{13}$$

$$\delta = (2.9 - a/\lambda_0) / 400 \text{ for } a/\lambda_0 \ge 0.1 \tag{14}$$

and

$$k_1 = 0.5\,(15 - a/\lambda_0) \text{ for } a/\lambda_0 \le 0.2 \tag{15}$$

$$k_1 = 0.2\,(15 - 17\, a/\lambda_0) \text{ for } a/\lambda_0 \ge 0.2 \tag{16}$$

δ_1 is the value of δ at $z = L$ in Fig.1.

The H-plane pattern may be obtained by setting $\phi = 0^\circ$, and the E-plane pattern by setting $\phi = 90^\circ$ in (3) and (4).

Array Factor of Circular Array

The circular array of isotropic radiators is shown in Fig.2. Radius of the circle, ρ_1 is

$$\rho_1 = N\lambda_0 / 2\pi \tag{17}$$

where N is the number of elements in the array and λ_0 is the wavelength.

Elements are placed at azimuthal angular intervals of 2π / N. The azimuthal angle ϕ_n of the n^{th} element is

$$\phi_n = \frac{2\pi n}{N} \tag{18}$$

Array factor, AF, of a circular array of N equally spaced elements may be written [1] as

$$AF=\sum_{n=1}^{N} I_n \exp\{j[\beta_0\rho_1 \sin\theta\cos(\phi - \phi_n)+\alpha_n]\} \tag{19}$$

where I_n = amplitude excitation of the n^{th} element,

α_n = phase excitation of the n^{th} element,

and

$\beta_0 = 2\pi / \lambda_0$ is the phase constant.

For uniform amplitude excitation of each element $I_n=I_o$, a constant. To direct the maximum of the main beam in the (θ_o, ϕ_o) direction, α_n may be chosen to be

$$\alpha_n = -\beta_0\rho_1 \sin\theta\cos(\phi_0 - \phi_n) \tag{20}$$

In Fig.2,

$$R_n = r - \rho_1 \cos(\psi_n) \tag{21}$$

where r is the distance from origin to point 'P', ρ_1 is radius of circle, and ψ_n is the progressive phase between the elements in the array.

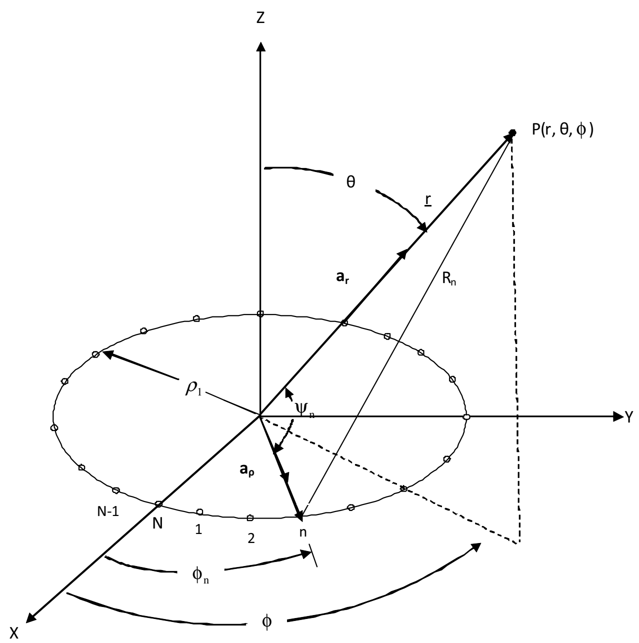

Figure 2: Geometry of circular array of N elements.

Circular Array of Nylon Rod Antennas

The tapered Nylon rod antennas, with feed end diameter equal to 0.025m are used as radiating elements in the array. The elements are uniformly spaced with a centre to centre spacing of λ_0 m between the elements. The radius of the array to place N number of elements without overlapping is then given by

$$\rho_1 = N\lambda_0 / 2\pi \tag{22}$$

with this radius the array factor can be computed using(19).

Total field, E, of the array can be computed using the principle of pattern multiplication as:

$$E = E\ (\text{Field of Single element}) \times \text{Array Factor} \tag{23}$$

The components of E radiated by a single Nylon rod antenna are given by (3) and (4) and the array factor is given by (19). The principle plane patterns are computed using (23). Software has been implemented in matlab to plot the radiation patterns.

Results and Discussion

Circular array of tapered Nylon rod antennas of length (L) equal to $6\lambda_0$, and taper angle (θ_1) equal to 2.5° is considered, to compute the principal plane patterns of the array at a frequency of 10 GHz or λ_0=0.03m. The elements are uniformly placed around the circumference of the circle. The number of elements is varied from 8 to 28 with an increase of 4. The principal plane patterns are computed for each set of elements and HPBW, SLL, and D_0 are computed for each set of elements and results are presented in Table-1.The Directivity may be computed using Kraus's formula [1]:

$$\text{Directivity}\,(D_0) = 41253/\,(\theta_E \times \theta_H) \tag{23}$$

Where

θ_E = HPBW in E-Plane (degrees)

θ_H = HPBW in H-Plane (degrees)

From the results presented in Table-1, it may be observed that, with increasing number of elements in the array the directivity as well as side lobe level increase, and it may also be observed that N=16, may be considered as an optimum choice, because in this case directivity is 30.52 dB and side lobe level is -9.9 dB. In all other cases, even though directivity is high, the SLL is slightly higher compared with N=16 case. The 3D radiation pattern for optimum choice is shown in Fig. 3. The principle plane patterns for optimum choice of elements are shown in Fig.4.

Table 1: Variation of HPBW, SLL, and D_0 with number of elements.

S.No.	Number of Elements(N)	Radius of the array in cm	HPBW (Deg.)		SLL (dB)		D_0 (dB)
			$\phi=0^\circ$	$\phi=90^\circ$	$\phi=0^\circ$	$\phi=90^\circ$	
1	8	$1.27\lambda_0$	11.2	11	-12.04	-13.98	25.25
2	12	$1.91\lambda_0$	8.2	8.2	-10.46	-11.06	27.88
3	16	$2.54\lambda_0$	6	6.1	-9.37	-9.9	30.52
4	20	$3.18\lambda_0$	4.8	4.6	-8.64	-9.12	32.72
5	24	$3.81\lambda_0$	4	4	-8.4	-8.64	34.11
6	28	$4.45\lambda_0$	3.4	3.4	-8.41	-8.64	35.52

Fig.3. 3D Radiation pattern of circular array of Nylon rod antennas

Figure 3: 3D Radiation pattern of circular array of Nylon rod antennas.

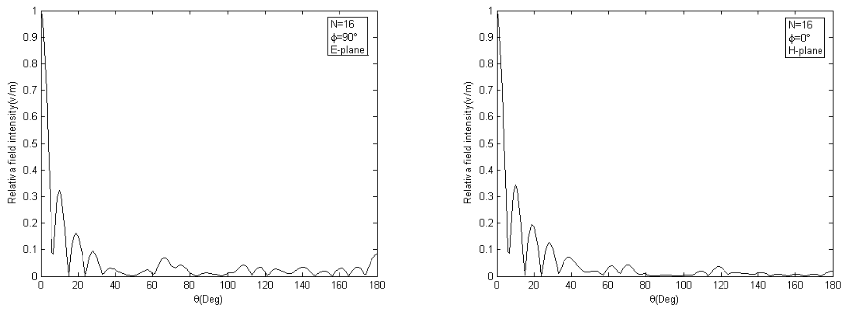

(a) (b)

Figure 4: Principal Plane patterns of circular array (N=16).

With a directivity of 30.52 dB and side lobe level of -9.9 dB, this array may be an attractive choice for radar applications.

List Symbols

Symbol	Meaning	Units
f	Frequency	Hertz
λ_o	Free space wave length	Meters
ε	Permittivity of medium	Farads per meter
μ	Permeability of medium	Henries per meter
β_o	Phase shift constant of free space	Radians
β	Phase constant of guided waves inside the dielectric rod antenna	Radians
β_1	Value of β at $z = L$ in Fig 1.	Radians
η_o	Free space wave impedance	Ohms
η_1^e	Wave impedance of electric field component	Ohms
η_1^m	Wave impedance of magnetic field component	Ohms
ρ_1	Radius of circle in the array	cm
N	Total number of elements in the array	
ψ_n	Progressive phase shift between the elements	Degrees
a_r	Unit vector in the direction of r	cm
a_ρ	Radial unit vector in the direction of ρ_1	cm
x, y, z	Rectangular coordinates	
ρ, ϕ, z	Cylindrical coordinates	
r, θ, ϕ	Spherical coordinates	

References

[1] Constantine A. Balanis, 2002, "Antenna Theory Analysis and Design", 2nd edition, John wiley & Sons Inc., pp 324-328.

[2] Rodney G. Vaughan, J. Bach Anderson and M.H. Langhorn, 1988, "Circular array of outward sloping monopoles for Vehicular Diversity Antennas", IEEE Trans. Antennas propagation, Vol.36, No.10, pp 1365-1374.

[3] Ronaold W.P. King, 1989, "Supergain antennas and the Yagi and circular arrays", IEEE Trans. Antennas propagation, Vol.37, No.2, pp178-186.

[4] Song Lizhong, Maning, Li Chongshen and Wuqum, 2008 "simulation and analysis of a microstrip circular array antenna at 15 GHz", IEEE Xplore,

[5] Naveen Kumar Saxena and Dr. P.K.S. Pourush, 2009, "Circular array of Triangular patches as filter", IEEE Xplore.

[6] Dr. J. Subramanyam and M.V.S. Prasad, 2009, "Radiation from tapered Nylon Rod Antennas – A Computational study". ICFAI Journal of Electrical and Electronics Engineering, vol. II, issue no.3, pp. 14-24.

[7] D.G. Kiely, "Dielectric Aerials", 1st edition, 1953, Mathuen & Co Limited, London, page 41.

[8] Anand Kumar, R. Chatterjee, 1968, "Radiation from tapered Dielectric Rod Aerials", IISC Journal, vol.50, issue no.4, pp. 374-392.